WILEY-VCH



ADVANCED SCIENCE
Open Access

# Supporting Information

for *Adv. Sci.*, DOI: 10.1002/advs.202002630

# Three-Phase Electrolysis by Gold Nanoparticle on Hydrophobic Interface for Enhanced Electrochemical Nitrogen Reduction Reaction

*Junchang Zhang, Bo Zhao, Wenkai Liang, Genshu Zhou, Zhiqiang Liang, Yawen Wang, Jiangying Qu,* Yinghui Sun,* Lin Jiang**

WILEY-VCH



# Supporting Information

Three-phase electrolysis by gold nanoparticle on hydrophobic interface for enhanced electrochemical nitrogen reduction reaction

*Junchang Zhang, Bo Zhao, Wenkai Liang, Genshu Zhou, Zhiqiang Liang, Yawen Wang, Jiangying Qu,* Yinghui Sun,* Lin Jiang**

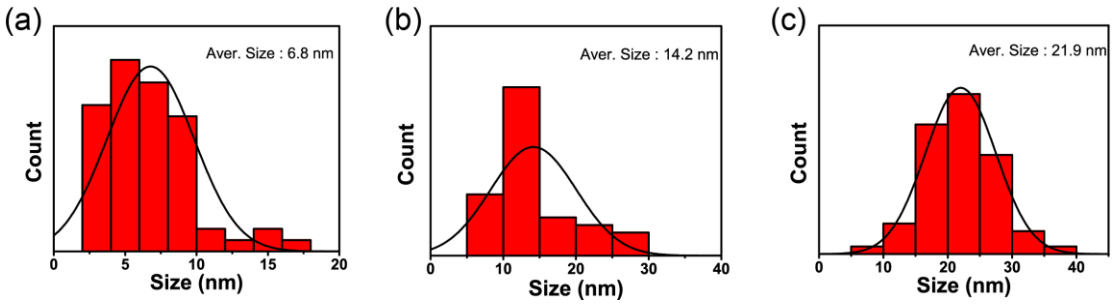


**Figure S1**. Size distribution diagram of Au NPs at different synthesis conditions of (a) 5 mM 15 μL, (b) 5 mM 45 μL and (c) 5 mM 75 μL.

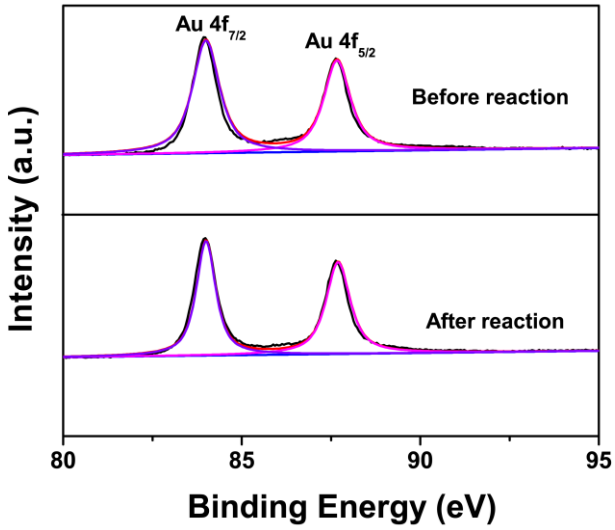


**Figure S2**. XPS spectrum of Au NPs in the Au 4f region before reaction and after 24-h electrolysis.

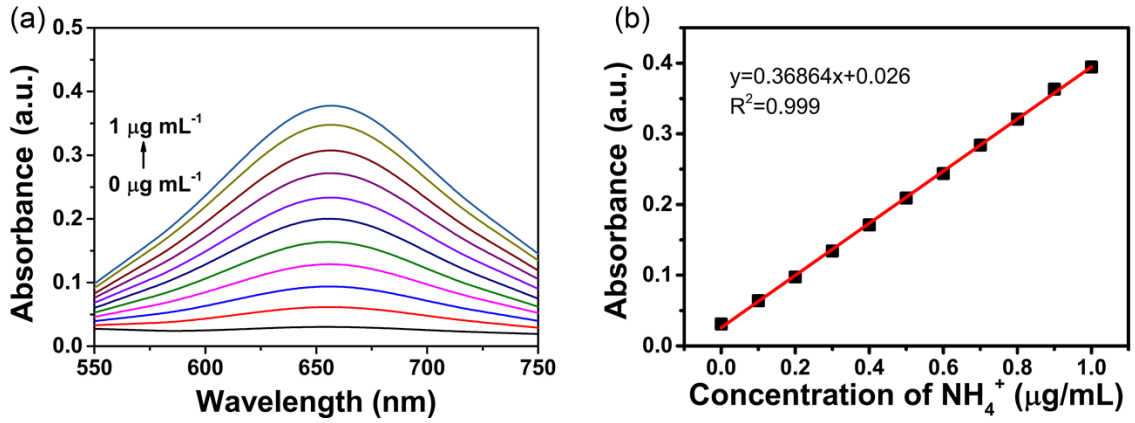


**FS3.** The UV-Vis absorption spectra and corresponding calibration curves for the colorimetric $NH_3$ assay using the indophenol blue method in 0.1 M $Na_2SO_4$.

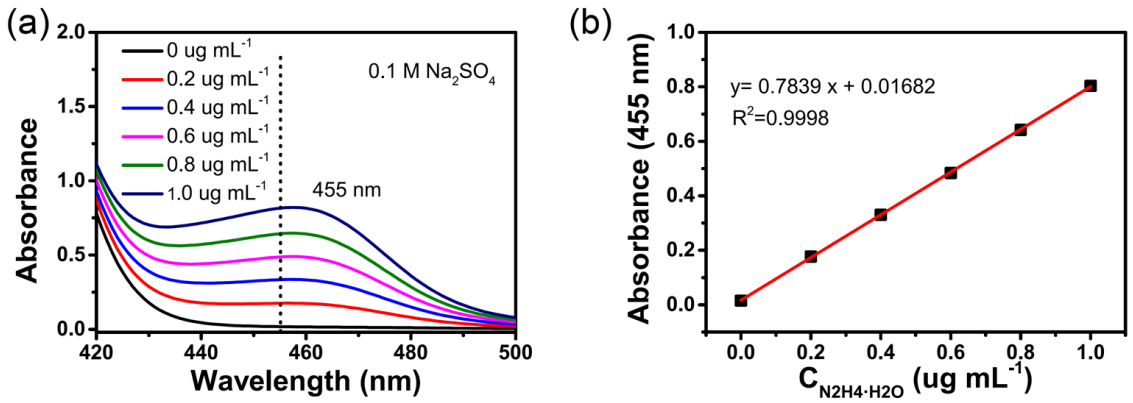


**Figure S4**. (a) The UV-Vis absorption spectra and (b) corresponding calibration curve for the colorimetric $N_2H_4$ assay in 0.1 M $Na_2SO_4$.

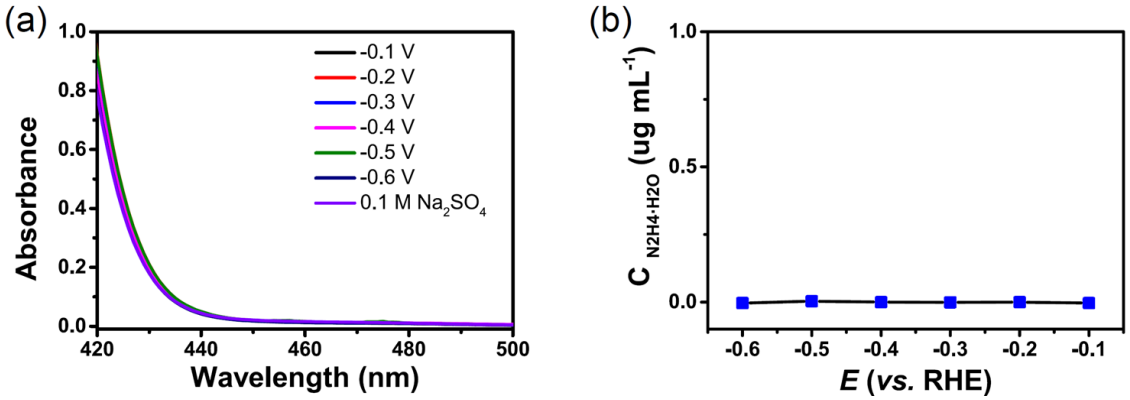


**Figure S5**. (a) The UV-Vis absorption spectra and (b) corresponding yield rate of $N_2H_4{\cdot}H_2O$ formation at selected potentials.

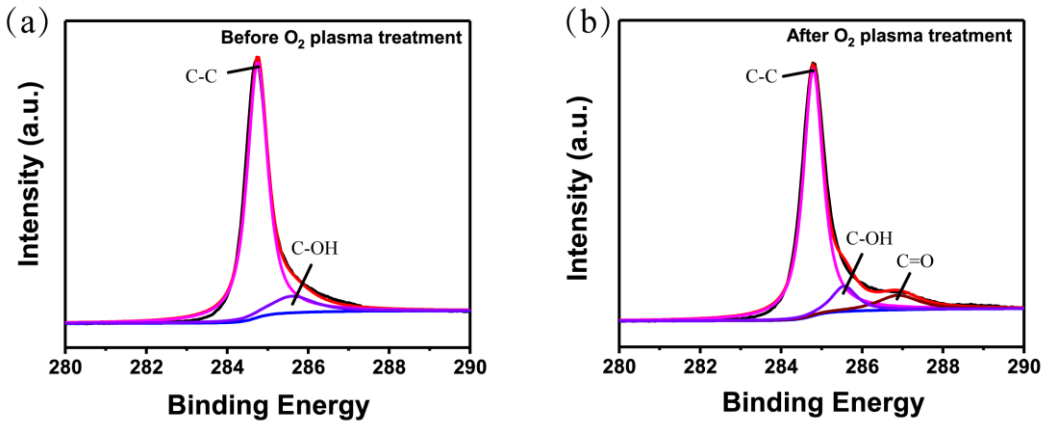


**Figure S6**. XPS spectrum of Au/CFP in the C region (a) before and (b) after $O_2$ treatment.

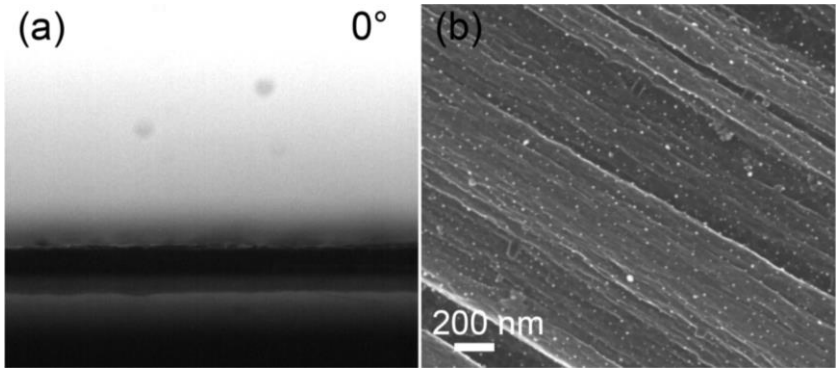


**Figure S7.** (a) The contact angle of Au/i-CFP and (b) The SEM image of Au/i-CFP.

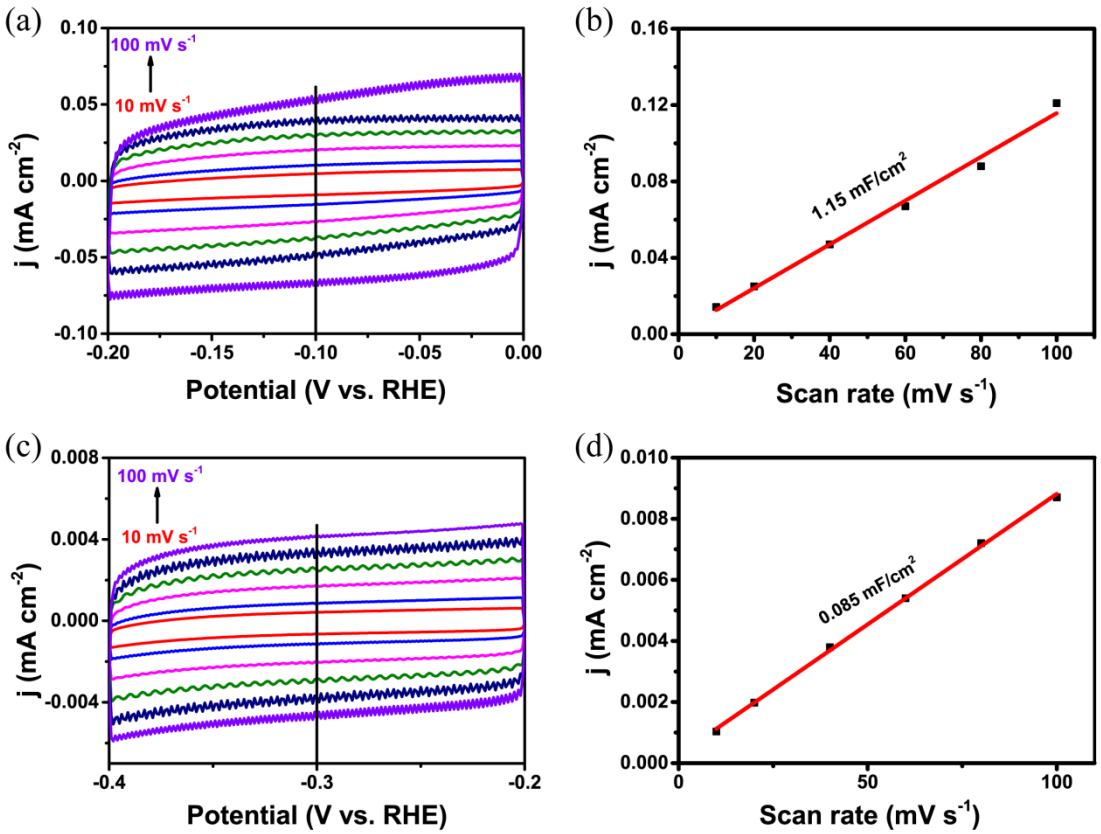


**Figure S8.** CV curves of Au/i-CFP (a) and Au/o-CFP (c) in the range of -0.2 and -0.4 V under Ar condition. Capacitive current densities at -0.3 V derived from CV curves against scan rates for Au/i-CFP (b) and Au/i-CFP (d).

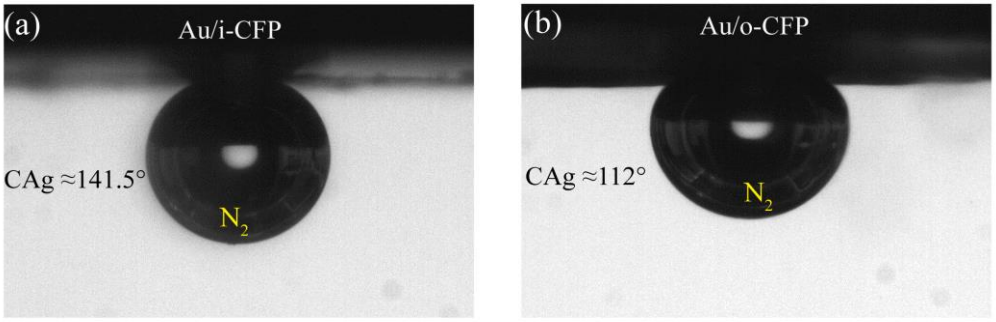


Figure S9. The shapes of $N_2$ bubble on the surface of Au/i-CFP (a) and Au /o-CFP (b) underwater.

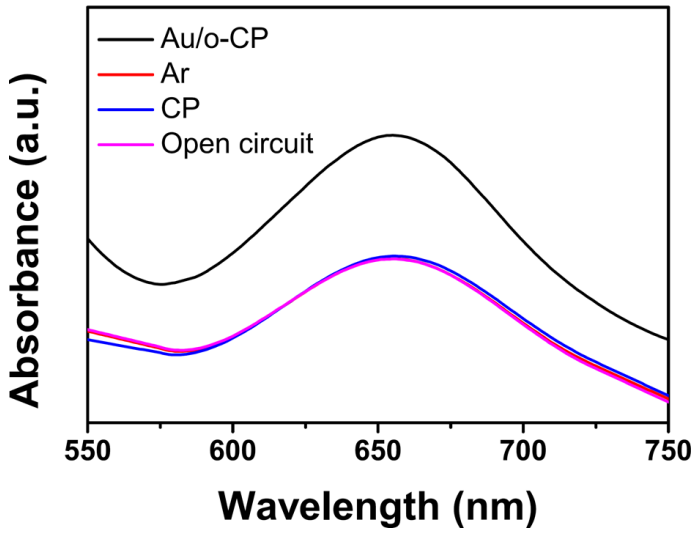


**Figure S10**. UV-Vis absorption spectra of the electrolytes stained with indophenols indicator under different conditions.

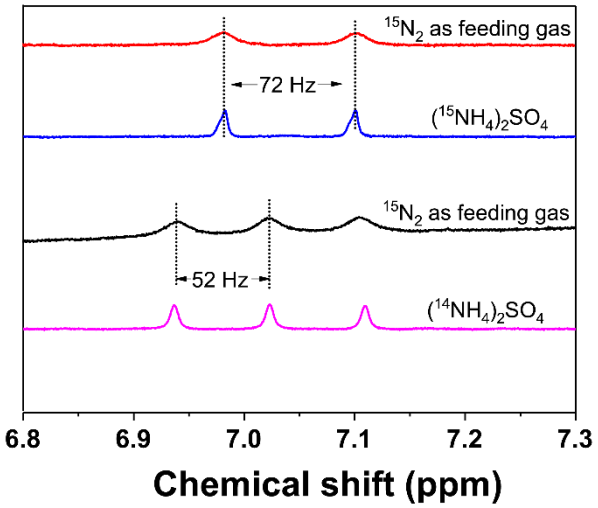


**Figure S11**. $^{15}N$ isotope labelled tests. $^{1}H$ NMR spectra for $(^{14}NH_4)_2SO_4$, $(^{14}NH_4)_2SO_4$ and the electrolyte after 6-h electrolysis with $^{14}N_2$ and $^{15}N_2$ as the feeding gases.

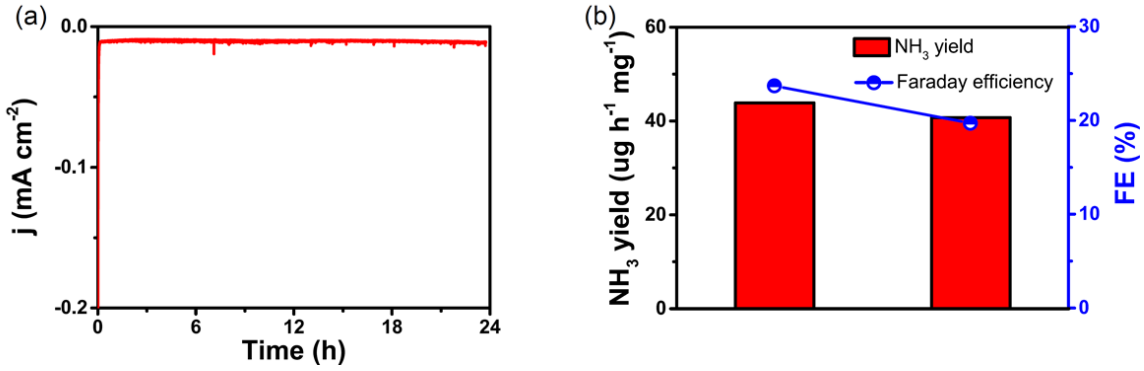


**Figure S12**. (a) The long time stability test of Au/o-CFP for 24 h and (b) corresponding their $NH_3$ yield rate and FE.

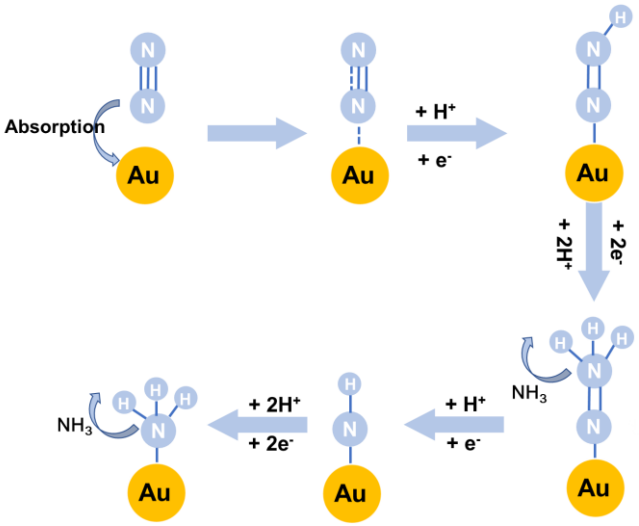


**Figure S13**. The possible NRR pathway for NRR on the Au surface.

**Table S1.** Comparison of the NRR performance for Au/o-CFP with recently reported NRR electrocatalysts under ambient conditions.

| Catalyst | Electrolyte | $NH_3$ yield rate | FE (%) | Ref. |
|---|---|---|---|---|
| **Au/o-CFP** | **0.1 M $Na_2SO_4$** | **40.6 μg $h^{-1}$ $mg^{-1}_{cat.}$** | **31.3** | **This work** |
| $Cu/TiO_2$ | 0.5 M $LiClO_4$ | 21.31 μg $h^{-1}$ $mg^{-1}_{cat.}$ | 21.99 | [1] |
| B-Ag NSs | 0.1 M HCl | 26.48 μg $h^{-1}$ $mg^{-1}_{cat.}$ | 8.86 | [2] |
| Au-$TiO_2$ sub-nanocluster | 0.1 M HCl | 21.4 μg $h^{-1}$ $mg^{-1}_{cat.}$ | 8.11 | [3] |
| Porous Au/Ni foam | 0.1 M $Na_2SO_4$ | 29.43 μg $h^{-1}$ $mg^{-1}_{cat.}$ | 13.36 | [4] |
| $Au/Ti_3C_2$ | 0.1 M $Na_2SO_4$ | 23 μg $h^{-1}$ $mg^{-1}_{cat.}$ | 34 | [5] |
| Nanoporous Au@ZIF | 0.1 M $Na_2SO_4$ | 28.7 μg $h^{-1}$ $mg^{-1}_{cat.}$ | 44 | [6] |
| PdRu tripods | 0.1 M KOH | 37.23 μg $h^{-1}$ $mg^{-1}_{cat.}$ | 1.85 | [7] |
| α-Au/CeOx-RGO | 0.1 M HCl | 8.3 μg $h^{-1}$ $mg^{-1}_{cat.}$ | 10.10 | [8] |

| | | | | |
|---|---|---|---|---|
| Au flower | 0.1 M HCl | 25.57 μg $h^{-1}$ $mg^{-1}_{cat.}$ | 6.05 | [9] |
| PdRu BPNs | 0.1 M HCl | 25.92 μg $h^{-1}$ $mg^{-1}_{cat.}$ | 1.53 | [10] |
| Ru SAs/g-$C_3N_4$ | 0.5 M NaOH | 23.0 μg $h^{-1}$ $mg^{-1}_{cat.}$ | 8.3 | [11] |
| Body‐centered cubic PdCu | 0.5 M LiCl | 35.7 μg $h^{-1}$ $mg^{-1}_{cat.}$ | 11.5 | [12] |
| PdO/Pd | 0.1 M NaOH | 18.2 μg $h^{-1}$ $mg^{-1}_{cat.}$ | 11.5 | [13] |
| $Ag_3Cu$ | 0.1 M $Na_2SO_4$ | 24.59 μg $h^{-1}$ $mg^{-1}_{cat.}$ | 13.28 | [14] |

**Table S2**. The average loading mass of Au NPs with different size detected by ICP-MS.

| Samples | Au (6.76 nm) | Au (14.2 nm) | Au (21.9 nm) |
|---|---|---|---|
| Average loading mass (μg) | 12.767 | 30.760 | 55.06 |

## References


[1] T. W. Wu, H. T. Zhao, X. J. Zhu, Z. Xing, Q. Liu, T. Liu, S. Y. Gao, S. Y. Lu, G. Chen, Abdullah M. Asiri, Y. N. Zhang, X. P. Sun, *Adv. Mater.* **2020**, 2000299.

[2] Y. Li, H. Yu, Z. Wang, S. Liu, Y. Xu, X. Li, L. Wang, H. Wang, *Chem. Commun.* **2019**, 55, 14745.

[3] M. M. Shi, D. Bao, B. R. Wulan, Y. H. Li, Y. F. Zhang, J. M. Yan, Q. Jiang, *Adv. Mater.* **2017**, 29, 1606550.

[4] H. Wang, H. Yu, Z. Wang, Y. Li, Y. Xu, X. Li, H. Xue, L. Wang, *Small* **2019**, 15, 1804769.

[5] D. Liu, G. Zhang, Q. Ji, Y. Zhang, J. Li, *ACS Appl. Mater. Interfaces* **2019**, 11, 25758.

[6] Y. Yang, S. Q. Wang, H. Wen, T. Ye, J. Chen, C. P. Li, M. Du, *Angew. Chem. Int. Ed.* **2019**, 131, 15506.

[7] H. Wang, Y. Li, C. Li, K. Deng, Z. Wang, Y. Xu, X. Li, H. Xue, L. Wang, *J. Mater. Chem. A* **2019**, 7, 801.

[8] S. J. Li, D. Bao, M. M. Shi, B. R. Wulan, J. M. Yan, Q. Jiang, *Adv. Mater.* **2017**, 29, 1700001.

[9] Z. Wang, Y. Li, H. Yu, Y. Xu, H. Xue, X. Li, H. Wang, L. Wang, *ChemSus*C*hem* **2018**, 11, 3480.

[10] Z. Wang, C. Li, K. Deng, Y. Xu, H. Xue, X. Li, L. Wang, H. Wang, *ACS Sustain. Chem. Eng.* **2018**, 7, 2400.

[11] B. Yu, H. Li, J. White, S. Donne, J. Yi, S. Xi, Y. Fu, G. Henkelman, H. Yu, Z. Chen, *Adv. Funct. Mater.* **2019**, 1905665.

[12] W. Tong, B. Huang, P. Wang, L. Li, Q. Shao, X. Huang, *Angew. Chem. Int. Ed.* **2019**, DOI:10.1002/anie.201913122.

[13] J. Lv, S. Wu, Z. Tian, Y. Ye, J. Liu, C. Liang, *J. Mater. Chem. A* **2019**, 7, 12627.

[14] H. Yu, Z. Wang, D. Yang, X. Qian, Y. Xu, X. Li, H. Wang, L. Wang, *J. Mater. Chem. A* **2019**, 7, 12526.